EARTHQUAKE ENGINEERING AND STRUCTURAL DYNAMICS, VOL. 23, 137 152 (1994)

ITERATIVE METHODS FOR NON-CLASSICALLY DAMPED DYNAMIC SYSTEMS

FIRDAUS E. UDWADIA[1] AND RAVI KUMAR[2]

Department of Civil Engineering, University of Southern California, Los Angeles, CA 90089-1453, U.S.A.

SUMMARY

Non-classically damped structural systems do not easily lend themselves to the modal superposition method because these systems yield coupled second-order differential equations. In this paper, a variety of new computationally efficient iterative methods for determining the response of such systems are developed. The iterative approaches presented here differ from those presented earlier in that they are computationally superior and/or are applicable to the determination of the responses of broader classes of structural systems. Numerical examples, which are designed to evaluate the efficacy of these schemes, show the vastly improved rates of convergence when compared to earlier iterative schemes.

1. INTRODUCTION

Recently, there has been a strong revival of interest in determining the response of non-classically damped structural systems. These systems are modelled by the following linear second-order differential equations of motion:

$$M\ddot{x}(t) + C\dot{x}(t) + Kx(t) = a(t), \quad x(t_0) = x_0, \ \dot{x}(t_0) = \dot{x}_0, \ t \in (t_0, T) \tag{1}$$

where the constant $N \times N$ matrices M, K and C are the mass, the stiffness and the damping matrices, respectively. The vectors $x(t)$ and $a(t)$ are $N \times 1$ vectors of displacement and force, respectively. For most of the physical systems arising in the area of structural dynamics, the mass matrix M is real, symmetric and positive-definite, and the stiffness matrix K is real, symmetric and positive-semidefinite. Under these circumstances, we can find a transformation matrix T which simultaneously diagonalizes M and K; for this transformation to diagonalize C also, the matrix C has to be of a special form.[1,2] In the literature this kind of damping is referred to as classical damping or proportional damping. The response of classically damped systems is obtained by the modal superposition method.

Yet in practice, proportional damping is usually a rare occurrence rather than a common one. This is because most large-scale, real-life, dynamic systems, are comprised of different subcomponents. Even if we were to ascribe a viscous damping character to each of these subcomponents, the final damping matrix C, constructed through, say, a finite element model for the whole system, would generally be of the non-proportional type. This would of course be more so true when these subcomponents themselves are comprised of widely differing materials, as is found, for example, in the area of soil–structure interaction, and in the area of aerospace structures (which are usually optimized for their weight).

In this paper, we assume that C is a real general matrix. When the matrices M, K and C cannot be simultaneously diagonalized by a suitable matrix transformation, one is left with the following coupled set of second-order linear differential equations

$$\ddot{z}(t) + F\dot{z}(t) + \Lambda z(t) = h(t), \quad z(t_0) = z_0, \ \dot{z}(t_0) = \dot{z}_0, \ t \in (t_0, T) \tag{2}$$

where $h(t) = T^{\mathrm{T}}a(t)$. The matrix T has columns which are the eigenvectors of the undamped system; the

[1] Professor.
[2] Graduate student.

0098–8847/94/020137–16$13·00

Received 11 June 1992
Revised 4 May 1993

damping matrix F, in general, is now a full matrix, and the diagonal matrix $\Lambda = \text{diag}(\lambda_1, \lambda_2, \ldots, \lambda_N)$, where $\lambda_1, \lambda_2, \ldots, \lambda_N$ are the eigenvalues of undamped system. Over the years, a considerable amount of research effort has been expended in the determination of the response of such MDOF systems whose damping is of non-classical type. The reader may refer to the extensive literature survey on this topic provided in Udwadia and Esfandiari.[3]

Here we present some important themes of research which have appeared since then. Shahruz and Langari[4] have studied the errors introduced in the system response due to decoupling which is achieved simply by ignoring off-diagonal terms of the damping matrix F. They have given the conditions under which the solution of this approximately decoupled system is 'close' to the solution of the coupled system. Shahruz and Packard[5] have further investigated the errors that can arise in lightly damped systems under harmonic excitations when some of the undamped natural frequencies of the system are close to the excitation frequency. Felszeghy[6] has given a method to obtain an approximate solution of equation (2). His method searches for another co-ordinate system in the neighbourhood of the normal co-ordinate system so that in the new co-ordinate system, removal of the coupling terms in the equations of motion produces a local minimum of the norm of the relative error. Claret and Venancio-Filho[7] have used essentially the same iterative procedure as given by Udwadia and Esfandiari[3] for the dynamic analysis of non-classically damped systems. They show convergence for only rather restrictive situations; when the undamped natural frequencies are not closely clustered, the off-diagonal elements of the matrix F are small, and all the undamped natural frequencies are relatively large.

In their previous work, Udwadia and Esfandiari[3] had developed a scheme which uncouples the equations of motion of non-classically damped systems and computes the response iteratively. They show that convergence is guaranteed for certain classes of matrices even when the undamped natural frequencies may be relatively small and clustered. Yet their convergence results are pertinent to only those matrices F which are either strictly diagonally dominant or which belong to a special class of symmetric and positive-definite matrices.

In this paper, we introduce two different sets of iterative schemes for determining the response of non-classically damped dynamic systems. They are superior to the previously proposed scheme[3] in that they are applicable to a much wider class of matrices F, and/or are computationally more efficient. The range of applicability of both schemes has been significantly extended to include (a) irreducible and weakly diagonally dominant F matrices and (b) *all* symmetric and positive-definite F matrices. For the analytical results guaranteeing convergence of these iterative schemes along with estimates of the asymptotic rates of convergence, the reader may refer to Udwadia and Kumar.[8] Extensive numerical testing supports our analytical work. It is shown that these techniques work well for a variety of situations. The techniques are capable of handling any arbitrary forcing function $h(t)$ and also provide error bounds on the accuracy of the responses thus obtained. The first set of schemes results in an uncoupled set of equations; it thus yields additional insights into the physics of the structural response. The second set of schemes while not uncoupling the system, is, in general, computationally far superior to the first.

Section 2 presents the basic underlying iterative approach for both sets of schemes. Using pseudo-code, algorithms are also presented for better understanding and implementation. Section 3 contains some numerical examples to show the validity of the proposed methods. For the different cases covered in the paper, it is shown that the second set of schemes converges faster than the first. The examples considered have been chosen with considerable care, in the sense that these examples when handled by the usual uncoupling techniques used to date, have presented some measure of difficulty to previous investigators. Finally, we discuss and compare these two sets of schemes. We also compare them with some of the previously proposed iterative methods.

2. ITERATIVE SCHEMES

We start from equation (2) by partitioning matrix F as

$$F = \alpha D + A + B \tag{3}$$

where $D = \text{diag}(d_1, d_2, \ldots, d_N)$ is the diagonal matrix obtained by taking the diagonal elements of matrix F,

and the real parameter α ($\alpha \neq 0$) is as yet unspecified. Substituting this decomposition of the matrix F in equation (2), we get

$$\begin{aligned} &\ddot{z}(t) + (\alpha D + A)\dot{z}(t) + \Lambda z(t) = h(t) - B\dot{z}(t) \\ &z(t_0) = z_0, \qquad \dot{z}(t_0) = \dot{z}_0, \qquad t \in (t_0, T) \end{aligned} \tag{4}$$

Our purpose is to generate a *cluster* of iterative schemes depending on (1) the specific split-down of the matrix F, i.e. the matrices chosen to be A and B and (2) the value of the parameter α chosen.

We first replace equation (4) by the following system:

$$\ddot{u}(t) + (\alpha D + A)\dot{u}(t) + \Lambda u(t) = f(t), \quad u(t_0) = z_0, \ \dot{u}(t_0) = \dot{z}_0, \ t \in (t_0, T) \tag{5}$$

where the function $f(t)$ is yet an unknown function. Let $\delta(t) = z(t) - u(t)$ denote the error vector in the responses determined from equations (4) and (5). Subtracting equation (5) from equation (4) we get

$$\begin{aligned} &\ddot{\delta}(t) + (\alpha D + A)\dot{\delta}(t) + \Lambda\delta(t) = h(t) - B\dot{z}(t) - f(t) \\ &\delta(t_0) = \dot{\delta}(t_0) = 0, \quad t \in (t_0, T) \end{aligned} \tag{6}$$

Since equation (6) is a second-order linear differential equation with zero initial conditions, we can conclude that $\delta(t) = 0$, $t \in (t_0, T)$ for all functions, $h(t)$, if and only if the right-hand side of equation (6) is zero, i.e.

$$f(t) = h(t) - B\dot{z}(t) \tag{7}$$

This implies that the solution of equations (2), (4) and (5) will be identical, i.e. $z(t) = u(t)$, for all t, *if and only if* $f(t)$ is as defined in equation (7). The only difficulty involved is that the time derivative of the response $z(t)$ is not known and, in fact, is obtained through the solution of equation (2), which is what we want to solve for, in the first place.

To overcome this problem, we consider the following iterative procedure which uses successive approximations for $\dot{z}(t)$. The scheme can be best described in the following algorithmic form where the superscript 'n' denotes quantities related to the nth iteration.

Step 1: **Set** $t_i = t_0$, $t_e = T$

$$u(t_i) = z_0, \ \dot{u}(t_i) = \dot{z}_0$$

Step 2: **Set** $n = 1$

$$\hat{f}^{(0)}(t) = h(t), \ t \in (t_i, t_e)$$

Step 3: **Solve** the system of equations (uncoupled or coupled depending on the scheme used)

$$\ddot{u}^{(n)}(t) + (\alpha D + A)\dot{u}^{(n)}(t) + \Lambda u^{(n)}(t) = \hat{f}^{(n-1)}(t), \ t \in (t_i, t_e)$$

Obtain:

$$\dot{u}^{(n)}(t), \ t \in (t_i, t_e)$$

Step 4: **Set** the following

$$\hat{f}^{(n)}(t) = h(t) - B\dot{u}^{(n)}(t), \ t \in (t_i, t_e)$$

Set $n = n + 1$

Step 5: **If** $\hat{f}^{(n)}(t)$ or $u^{(n)}(t)$ converges to the desired accuracy

Then

$$z(t) \cong u^{(n)}(t), \quad \dot{z}(t) \cong \dot{u}^{(n)}(t) \quad \textit{and} \quad f(t) \cong \hat{f}^{(n)}; \ t \in (t_i, t_e)$$

Stop

Else

Go to Step 3

Different iterative schemes can now be generated from the general procedure outlined above by making different choices of the matrices, A and B, and the parameter α. In the sequel we shall, in particular, concentrate on two specific sets of iterative schemes.

Scheme I: The parameters that define this scheme are as follows:

(1) $A = 0$ and
(2) $B = (1 - \alpha)D + P$, where the matrix P contains the off-diagonal terms of the matrix F and has zeros along the diagonal.

We note that different values of the parameter α will generate different iterative schemes, all belonging generically to Scheme I. Thus, the matrix F is split as

$$F = \alpha D + B := \alpha D + \{(1 - \alpha)D + P\} \tag{8}$$

Scheme II: The parameters that define this scheme are as follows:

(1) $A = L$, where L is the lower triangular part of the matrix F and
(2) $B = (1 - \alpha)D + U$, where U is the upper triangular part of the matrix F.

Again, different values of the parameter α will generate different iterative schemes all generically belonging to Scheme II. In this set of schemes the matrix F is split as

$$F = \alpha D + A + B := \alpha D + L + (1 - \alpha)D + U \tag{9}$$

We point out that the preliminary paper by Udwadia and Esfandiari[3] only deals with one element of the set provided by Scheme I, i.e. when α equals unity.

The following important points about these two sets of iterative schemes should be noted:

1. For Scheme I, at each iteration a set of uncoupled differential equations is solved (see Step 3, above). Scheme II has the computational advantage that it does not require the simultaneous storage of the two approximations $\dot{u}^{(n+1)}(t)$ and $\dot{u}^{(n)}(t)$ in the course of computation as does Scheme I. This saves a considerable amount of memory storage, specially for problems involving large matrices.
2. In Step 4 above, we have explicitly indicated the iterative approximations of $\hat{f}^{(n)}(t)$; the right-hand side of equation (5) will be referred to, in conformity with the work of Udwadia and Esfandiari,[3] as *the pseudo-force*.

The first set of iterative schemes shows that it may be possible to think of the response of the system represented by equation (2) as being separable into different 'modes' provided that it is subjected to the pseudo-force $f(t)$ rather than the actual forcing function $h(t)$. As pointed out in the work of Udwadia and Esfandiari,[3] unlike in this scheme, past efforts for uncoupling equation (2) have concentrated mainly on diagonalizing the damping matrix F without making appropriate modifications to the forcing function, $h(t)$, on the right-hand side of the equation. Without such an adjustment, it is obvious that, in general, inaccurate responses will result for non-classically damped systems.

We next demonstrate these iterative schemes on systems having different kinds of damping matrices F, namely, when F is (i) strongly diagonally dominant, (ii) irreducible and weakly diagonally dominant, and (iii) symmetric and positive-definite matrix. The conditions under which convergence to the exact response is guaranteed for these three kinds of matrices F, in other words, conditions under which the error vector $\delta^{(n)}(t) = z(t) - u^{(n)}(t) \to 0$ as $n \to \infty$, have been investigated in a rigorous manner in Udwadia and Kumar.[8] The reader may want to refer to Udwadia and Kumar[8] so that the significance of the numerical examples can be better appreciated.

3. NUMERICAL RESULTS

This section covers some numerical results for non-classically damped systems to show the effectiveness of the two iterative schemes developed in the previous section. For the examples considered, the system responses are strongly coupled through the damping terms. Customary uncoupling methods in N-space fail miserably in these situations.[9,10] We find that in all examples studied, the iterated results, after only a few iterations are almost the same as those obtained from using the fourth-order Runge–Kutta integration scheme.[11] For all the matrices F which have been covered in our numerical examples, Scheme II converges faster than Scheme I. Some of the results produced here are corresponding to the approximate optimum values of the parameter α which make the bounds on the corresponding spectral radius a *minimum*.[8] The approximate optimum values of α for different kinds of matrices F are analytically obtained in Udwadia and Kumar.[8] It has also been verified through numerical experiments that these theoretical estimates of the approximate optimum values of α do yield rapid convergence.

The direct use of the fourth-order Runge–Kutta procedure to obtain response results requires approximately $(12N^2 + 18N)$ multiplications for each time step, where N is the number of equations. The iterative techniques, developed in this paper, utilize the Nigam–Jennings algorithm[12] for numerical integration. This algorithm requires $8N$ multiplications per iteration for each time step. In addition to this, Scheme I needs N^2 multiplications per iteration for each time step to uncouple the set of equations, i.e. to compute $[(1-\alpha)D + P]\dot{u}^{(n-1)}$. Scheme II also requires an additional N^2 multiplications per iteration per time step to compute $L\dot{u}^{(n)}$ and $[(1-\alpha)D + U]\dot{u}^{(n-1)}$. We note that these additional numbers of multiplications are the same for both the schemes. Thus, for each time step, a total of $(N^2 + 8N)I$ multiplications are required to obtain the response results, where I is the number of iterations. Hence for large N, when I is less than 12 for achieving the required convergence, the two iterative schemes developed herein become computationally efficient. Throughout this section it is assumed that the various parameter values are provided in consistent physical units.

Example 1

Consider the ten DOF system whose parameters are defined in the appendix. The initial time t_0 and final time T are taken to be zero and 10 units, respectively. The matrix F, chosen, is non-symmetric and strongly *diagonally dominant*.

It should be noted that the diagonal elements of matrix Λ (which correspond to the squares of the undamped natural frequencies of vibration) are clustered, several of them being equal to 20 units. The choice of identical values for these diagonal elements causes us to expect intense interaction[10] through the coupling created by the matrix F. This would be even more prominent because the excitation is also taken to have a frequency of $\sqrt{20}$ units.[13] We will see later that Examples 2 and 3 also have these critical features. Standard uncoupling methods used to date have been known to provide erroneous results in such situations.[10,13]

We define the normalized root mean square (RMS) error at the nth iteration in component i as

$$\text{normalized RMS error at iteration } n \text{ in component } i = \frac{\text{RMS of } \{u_i^{(n)} - z_i^{RK}\}}{\text{RMS of } \{z_i^{RK}\}} \tag{10}$$

where $u_i^{(n)}$ is the nth iterate of component i, and z_i^{RK} is the ith component of the response of equation (2) calculated using the Runge–Kutta integration scheme.

In this example as well as in Example 3, we have shown the graphs of the normalized RMS error for those components which converge most slowly among all the components. Therefore, the normalized RMS error (see e.g. Figures 1 and 2) in these components at various iterations gives the maximum error bound for other components at the corresponding iterations. The RMS values of the displacement responses obtained using the Runge–Kutta method are also provided in the figures. The stopping criterion for our iterative schemes is that the right-hand side of equation (10) be less than 10^{-5}. We have also provided the time history plots for the most slowly convergent velocity component for all the examples. These plots include exact results by the Runge–Kutta method and the results corresponding to the first iteration, and to some other iterations.

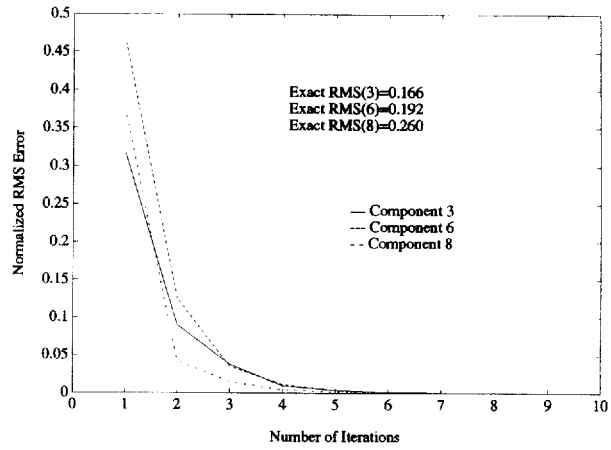

Figure 1. Normalized RMS error of displacement components 3, 6 and 8 (Example 1 (Scheme I)) versus number of iterations

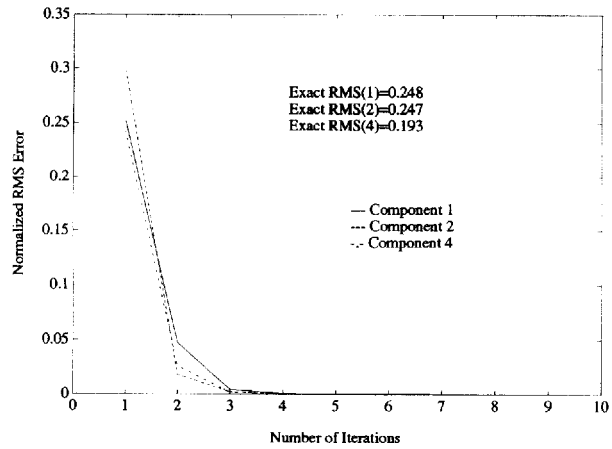

Figure 2. Normalized RMS error of displacement components 1, 2 and 4 (Example 1 (Scheme II)) versus number of iterations

In our numerical results, we have also given the estimates of average rates of convergence. In terms of actual computations, the significance of average rate of convergence,[14] R_{av}, is the following. The quantity

$$v \equiv \left(\frac{\| e^{(n)} \|}{\| e^{(0)} \|} \right)^{1/n} \tag{11}$$

is the average reduction factor per iteration for the successive error norms, where $\| e^{(n)} \|$ is the Euclidean norm of the error vector at nth iteration and $\| e^{(0)} \|$ is the Euclidean norm of initial error vector. The ith component of the error vector at the nth iteration is computed as

$$e_i^{(n)} = \left(\int_{t_0}^{T} \{ \delta_i^{(n)}(t) \}^2 \, \mathrm{d}t \right)^{1/2} \tag{12}$$

where $\delta_i^{(n)}(t)$ is the error in the ith component at the nth iteration.

Defining

$$R_{\text{av}} = -\frac{1}{n} \log \left[\frac{\| e^{(n)} \|}{\| e^{(0)} \|} \right] \tag{13}$$

as the average rate of convergence over n iterations,[14] from equation (11), we get

$$\nu = 10^{-R_{av}} \tag{14}$$

Again, defining $N_n \equiv R_{av}^{-1}$, we see from the previous equality that

$$\nu^{N_n} = 1/10 \tag{15}$$

so that N_n is a measure of the number of iterations required to reduce the Euclidean norm of the initial error vector by a factor of 10. We have compared the two iterative schemes on the basis of their average rates of convergence, R_{av}, over a specified number of iterations.

Figures 1 and 2 show the convergence pattern of representative displacement components, as mentioned previously, for Schemes I and II, respectively. Figure 3 shows the time history of velocity component 6 (for Scheme I) at the first and fourth iterations including the exact results obtained by the Runge–Kutta method. The results from the fourth iteration cannot be distinguished in the graph from those of the Runge–Kutta

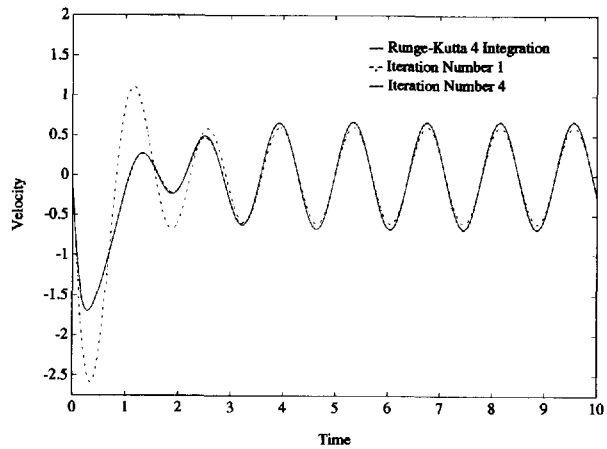

Figure 3. Time history of the velocity component 6 (Example 1 (Scheme I)) corresponding to the exact response, first and fourth iterations

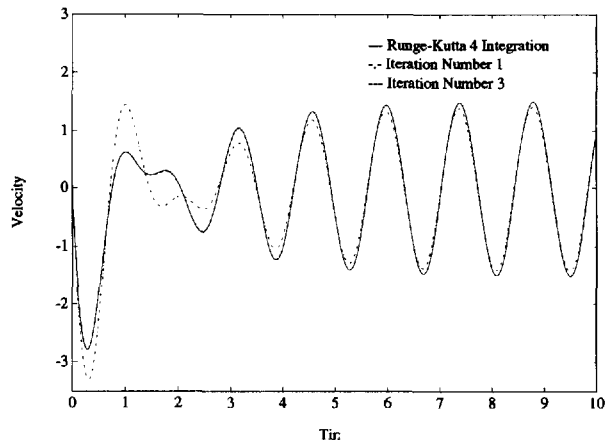

Figure 4. Time history of the velocity component 1 (Example 1 (Scheme II)) corresponding to the exact response, first and third iterations

method. Similarly, Figure 4 shows velocity component 1 at various iterations for Scheme II. The approximate optimum value of the parameter α, which has been used in this example, is 1·0. Also, the value of the parameter $\mu(=1/\alpha)$ for Scheme II has been taken as 1·0.[8] Note that in Scheme I when $\alpha = 1{\cdot}0$, the normalized RMS error which results at the first iteration provides a measure of the extent of the error in the system's response were all the off-diagonal terms of the matrix F ignored.

In this example, the average rates of convergence (R_{av}) for displacement components for Schemes I and II over 5 iterations (i.e. $n = 5$ in equation (11)) are 0·66 and 0·98, respectively. The reciprocal (N_n) of these average rates of convergence shows that Scheme I takes approximately 1·52 iterations to reduce the norm of the initial error vector by a factor 10, while Scheme II needs just 1·02 iterations to do the same. Hence, it can be concluded that for this case Scheme II converges approximately 1·5 times faster than Scheme I. The lower bound on the asymptotic rate of convergence (see Reference 8) for Scheme I turns out to be $7{\cdot}5 \times 10^{-3}$.

Example 2

Here we consider an irreducible and weakly diagonally dominant damping matrix F given as

$$F = \begin{bmatrix} 0{\cdot}40 & 0{\cdot}20 & 0{\cdot}20 \\ 0{\cdot}10 & 0{\cdot}60 & 0{\cdot}30 \\ 0{\cdot}10 & 0{\cdot}30 & 0{\cdot}50 \end{bmatrix} \quad \text{and} \quad \Lambda = \text{diag}\{20{\cdot}0, 20{\cdot}0, 20{\cdot}0\} \tag{16}$$

The parameters t_0 and T are taken to be zero and 10 units, respectively. The initial conditions are

$$z_i(0) = 0{\cdot}0, \quad i = 1, 2, 3, \quad \text{and} \quad \dot{z}_i(0) = 1{\cdot}0, \quad i = 1, 2, 3 \tag{17}$$

And the system is subjected to the forcing vector $h(t)$ given by

$$h_1(t) = 2\sin\sqrt{20}t, \qquad h_2(t) = -2\sin\sqrt{20}t, \qquad h_3(t) = 2\sin\sqrt{20}t, \quad t \in (0, 10) \tag{18}$$

Once again the undamped natural frequencies are taken to be identical. The frequency of excitation is taken to be the same as the undamped natural frequency to ensure intense interaction of the response through the coupling caused by the non-diagonal matrix F.

Parameter $\alpha = 1{\cdot}1$ and $\mu = 1{\cdot}0$ have been used for the computations.[8] Figures 5 and 6 show the convergence of the displacement components with increasing iteration numbers for the two iterative schemes. Figures 7 and 8 show the velocity component, $\dot{z}_2(t)$, at different iterations along with the exact response obtained by the Runge–Kutta method. The average rates of convergence over 5 iterations for Schemes I and II turn out to be 0·514 and 0·821, respectively. Thus, for this example Scheme II converges approximately 1·6 times faster than Scheme I.

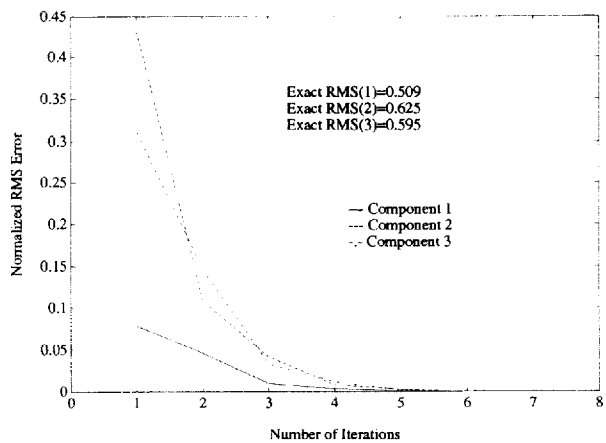

Figure 5. Normalized RMS error of displacement components 1, 2 and 3 (Example 2 (Scheme I)) versus number of iterations

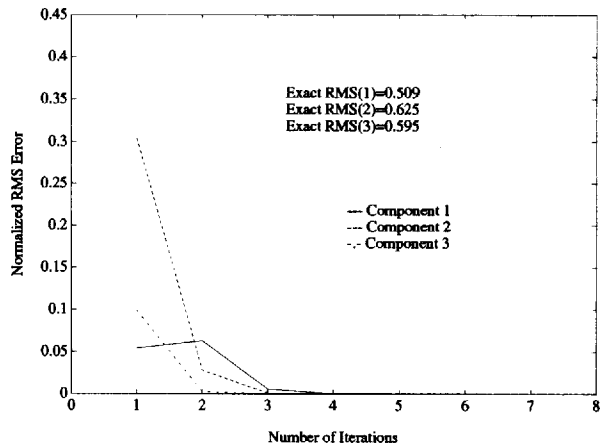

Figure 6. Normalized RMS error of displacement components 1, 2 and 3 (Example 2 (Scheme II)) versus number of iterations

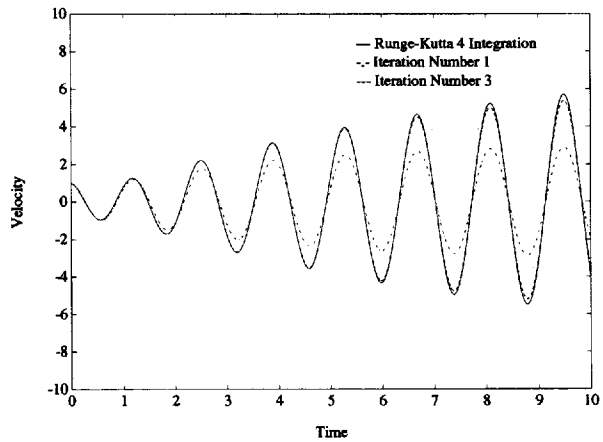

Figure 7. Time history of the velocity component 2 (Example 2 (Scheme I)) corresponding to the exact response, first and third iterations

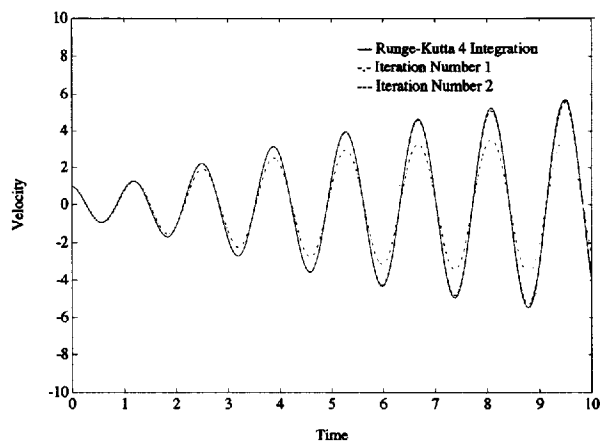

Figure 8. Time history of the velocity component 2 (Example 2 (Scheme II)) corresponding to the exact response, first and second iterations

Example 3

Let F be a symmetric and positive-definite matrix with the elements as defined in the appendix. The other parameters of the system are the same as in Example 1. Here it should be noted that F is no longer diagonally dominant. The minimum and maximum eigenvalues of matrix $D^{-1}F$ are 0·6904 and 2·0272, respectively, where D is the diagonal part of the matrix F. Therefore, convergence for Scheme I is guaranteed as long as $\alpha > 2{\cdot}0272/2$.[8] Here we have given the results for $\alpha = 1{\cdot}3588$, the approximate optimum value.[8] For Scheme II, convergence will occur if $0 < \mu < 1{\cdot}9066$ (see Reference 8), but for the computations the value of μ, which has been used, is 0·9713.

Figures 9 and 10 show the normalized RMS error versus iteration number for the representative displacement components for Schemes I and II, respectively. Figure 11 contains time history plots of velocity component 5 (the most slowly converging component) at the first and fourth iterations along with the exact time history obtained by the Runge–Kutta method. Similarly, Figure 12 shows velocity component 3 (the most slowly converging component) for Scheme II at different iterations. The average rates of convergence over 5 iterations for Schemes I and II, for the above-mentioned parameters, are calculated as 0·532 and 0·902, respectively. Thus, Scheme II converges approximately 1·7 times faster than Scheme I.

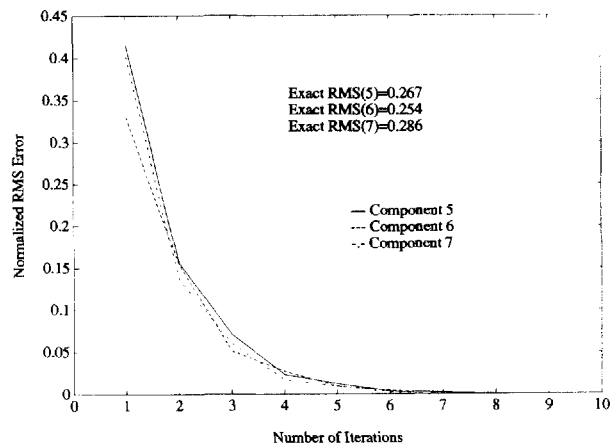

Figure 9. Normalized RMS error of displacement components 5, 6 and 7 (Example 3 (Scheme I)) versus number of iterations

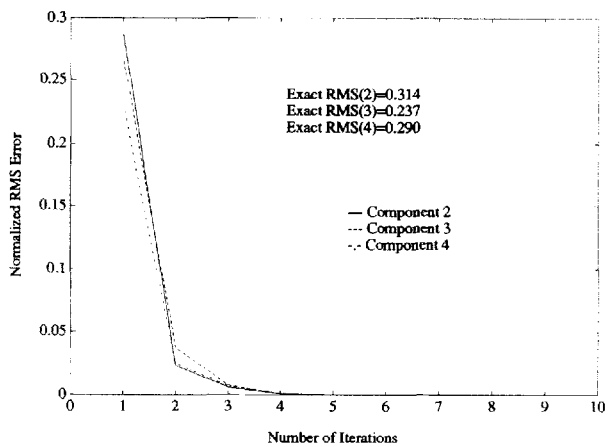

Figure 10. Normalized RMS error of displacement components 2, 3 and 4 (Example 3 (Scheme II)) versus number of iterations

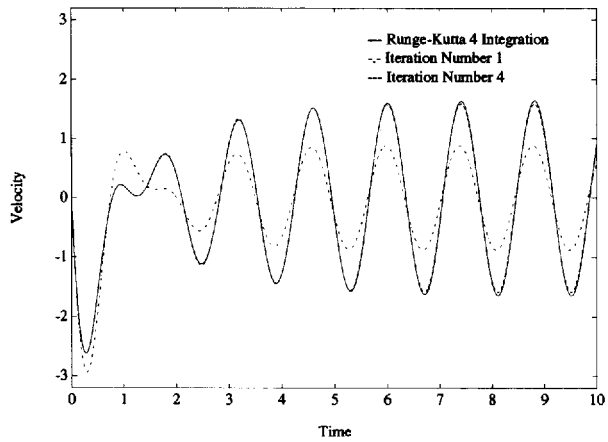

Figure 11. Time history of the velocity component 5 (Example 3 (Scheme I)) corresponding to the exact response, first and fourth iterations

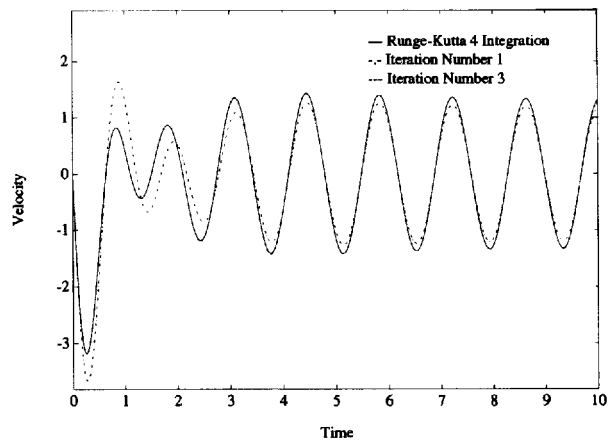

Figure 12. Time history of the velocity component 3 (Example 3 (Scheme II)) corresponding to the exact response, first and third iterations

Figure 13 shows the nature of convergence for Scheme I, for displacement components 4, 5 and 7, with $\alpha = 2{\cdot}7176$ (i.e. two times the approximate optimum value of α). Figure 14 shows the time history of velocity component 4 (the most slowly converging component) at the first and tenth iterations. Velocity response obtained by the Runge–Kutta method is also shown. The average convergence rate for this value of α, over 5 iterations, turns out to be $R_{av} = 0{\cdot}293$. This shows that choosing a value of α, which is two times the approximate optimum α slows down the convergence process by almost a factor of two (cf. Figures 9 and 13). The lower bound on the asymptotic rate of convergence for Scheme I, using the approximate optimum value of α, is computed as 0·308. Note that for this example, the iterative scheme given by Udwadia and Esfandiari[3] does not promise convergence because $\lambda_{max}(D^{-1}F) > 2$, where λ_{max} denotes the maximum eigenvalue.

Example 4

This example has been specially tailored to illustrate that (1) if matrix F is symmetric and positive-definite then for Scheme II to converge to the exact response the parameter μ needs careful selection and (2) that the iterative scheme in anomalous situations may be slow to converge. Let us consider the following symmetric

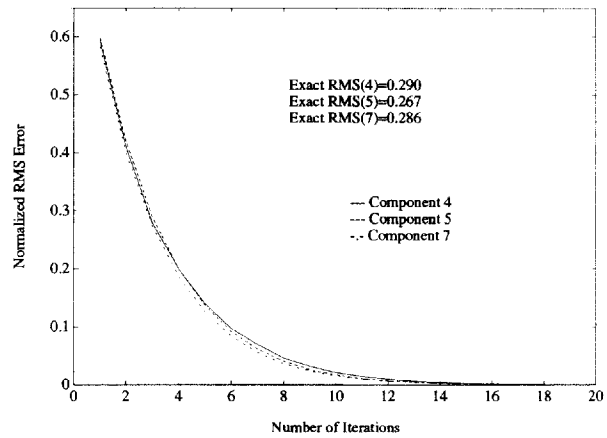

Figure 13. Normalized RMS error of displacement components 4, 5 and 7 (Example 3 ($\alpha = 2{\cdot}7176$)) versus number of iterations

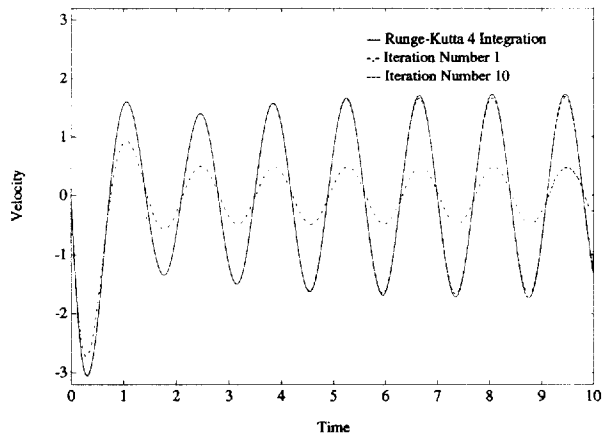

Figure 14. Time history of the velocity component 4 (Example 3 ($\alpha = 2{\cdot}7176$)) corresponding to the exact response, first and tenth iterations

and positive-definite matrix:

$$F = \begin{bmatrix} 1{\cdot}00 & 0{\cdot}99 & 0{\cdot}98 \\ 0{\cdot}99 & 1{\cdot}00 & 0{\cdot}99 \\ 0{\cdot}98 & 0{\cdot}99 & 0{\cdot}995 \end{bmatrix} \tag{19}$$

and

$$\Lambda = \text{diag}\,\{19{\cdot}0,\ 17{\cdot}0,\ 15{\cdot}0\} \tag{20}$$

with the initial conditions

$$z(0) = [-0{\cdot}19050,\ -0{\cdot}03600,\ -0{\cdot}02407]^{\mathrm{T}}$$

and (21)

$$\dot{z}(0) = [-3.9970,\ 4.6380,\ -0.7948]^{\mathrm{T}}$$

The parameters t_0 and T are taken to be zero and 80 units (s), respectively. The system is subjected to the same forcing vector, $h(t)$, as given in Example 2. Figure 15 shows the spectral radius $\rho_{S_{2;\mu}}(\omega)$ versus μ and the

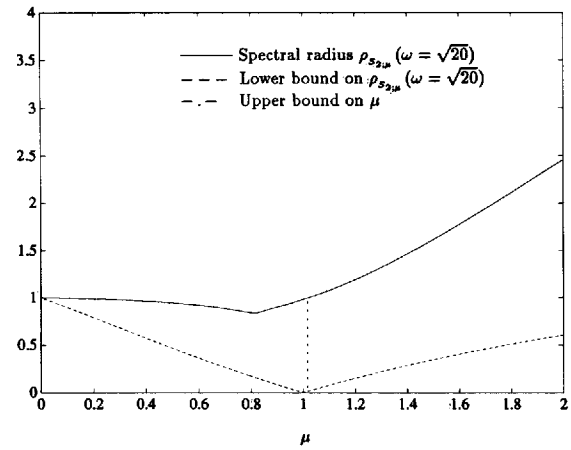

Figure 15. Spectral radius $\rho_{S_{2,\mu}}(\omega)$ and lower bound on the spectral radius versus parameter μ (Example 4)

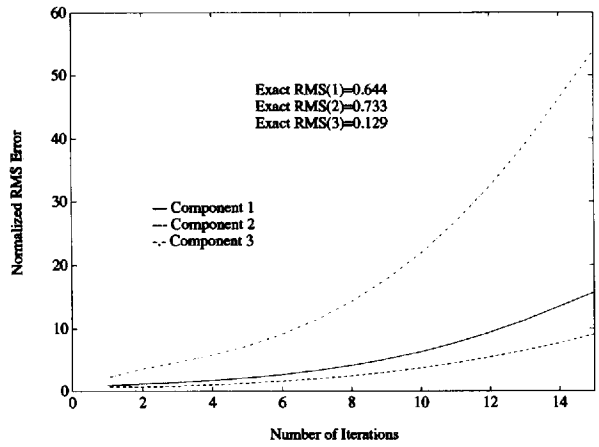

Figure 16. Normalized RMS error of displacement components 1, 2 and 3 (Example 4 (μ = 1·8)) versus number of iterations

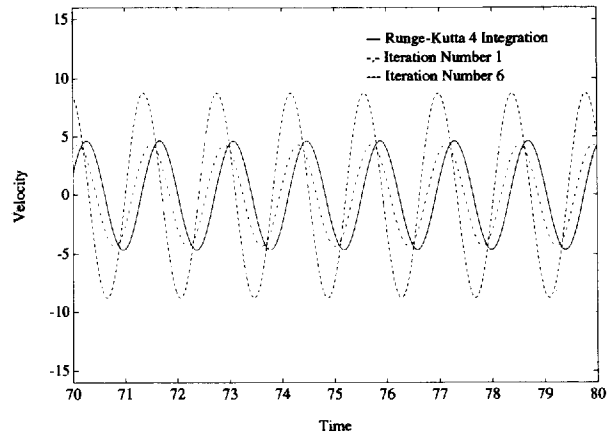

Figure 17. Time history of the velocity component 2 (Example 4 (μ = 1·8)) corresponding to the exact response, first and sixth iterations

lower bound on $\rho_{S_{2;\mu}}(\omega)$ versus μ for $\omega = \sqrt{20}$ units.[8] For $\omega = \sqrt{20}$ units, the value of the upper bound on μ (see Reference 8) sufficient for convergence turns out to be as $\mu = 1{\cdot}017$. Therefore, convergence is guaranteed as long as $0 < \mu < 1{\cdot}017$ and for $1{\cdot}017 \leqslant \mu < 2$, Scheme II may diverge.

Figure 16 shows some divergence results for the forcing function frequency $\omega = \sqrt{20}$ units. Here μ has been taken as 1·8, which is beyond the region of convergence, as explained earlier. Figure 17 shows the time history of velocity component 2, which is the most slowly divergent component, from 70 to 80 s at the first and sixth iterations. The response obtained from Runge–Kutta integration is also plotted.

Figure 18 shows the convergence pattern for this example when $\mu = 0{\cdot}82$, for all three displacement components. Figure 19 shows the time history of velocity component 3 for the first and 30th iterations. The average rate of convergence for $\mu = 0{\cdot}82$ has been estimated as 0·084 over 40 iterations. As is obvious from the rate of convergence and from Figures 18 and 19, the convergence for this case occurs very slowly. This example was constructed to show slow convergence, because the spectral radius of iteration matrix[8] is very close to unity. In the vast numerical experimentation that we have performed, this example, by construction, is anomalous in its slow rate of convergence.

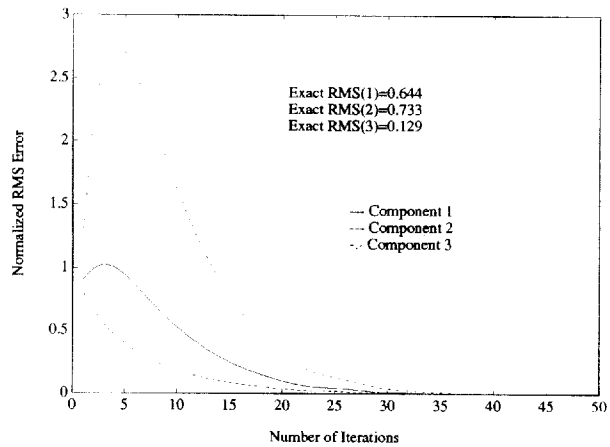

Figure 18. Normalized RMS error of displacement components 1, 2 and 3 (Example 4 ($\mu = 0{\cdot}82$)) versus number of iterations

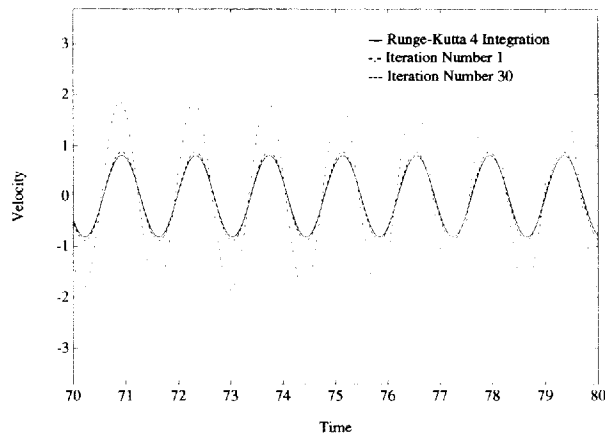

Figure 19. Time history of the velocity component 3 (Example 4 ($\mu = 0{\cdot}82$)) corresponding to the exact response, first and 30 iterations

4. CONCLUSIONS AND DISCUSSION

Two new, simple, and computationally efficient iterative methods are developed for the numerical solution of rather general, linear dynamic systems modelled by coupled differential equations. It is shown that these two techniques are better alternatives to the approximate and iterative methods that have so far been used. Rigorous results on when convergence is guaranteed may be found in Udwadia and Kumar.[8] Most previous investigators have focused on diagonalizing the damping matrix F by ignoring the off-diagonal elements so that the modal superposition method can be used. Since the right-hand sides of the equations of motion are kept intact, this leads to inaccurate response results. The iterative schemes presented in this paper show that by appropriately adjusting the right-hand side of equation (2) at each iteration, the exact solution can be rapidly obtained. The following points regarding these two sets of iterative schemes should be noted.

(i) Both the iterative schemes, are shown to converge for three different classes of matrices F: (a) strongly diagonally dominant matrices, (b) irreducible and weakly diagonally dominant matrices, and (c) symmetric and positive-definite matrices. These matrices cover a wide variety of problems encountered in the field of structural dynamics (see Reference 8 for sufficient conditions required for the convergence of these two schemes).

(ii) Scheme I decouples the set of normalized equations of motion and thus yields insights in the physics of the response of the structural systems.

(iii) For symmetric and positive-definite matrices F, the iterative scheme developed by Udwadia and Esfandiari[3] (which is a special case of Scheme I) guarantees convergence as long as $\lambda_{max}(D^{-1}F) < 2$, where matrix D contains diagonal elements of the matrix F. Scheme I, presented here, always provides convergence as long as α is chosen to be greater than $\lambda_{max}(D^{-1}F)/2$. Thus, the limitation imposed in Reference 3 has been removed.

(iv) In the case of strongly diagonally dominant, and symmetric and positive-definite matrices F, the relatively easy-to-compute approximate optimum values of the parameter α (which are developed in Reference 8) make Scheme I converge rapidly to the exact solution within a few iterations. For any arbitrary excitation, the convergence rates at these values of α appear to be the best achievable.

(v) Although Scheme II fails in uncoupling the system of equations, vast numerical experience shows that, in general, it is computationally far superior than Scheme I. In the examples considered in the previous section, it is observed that the convergence rate of Scheme II is approximately 1·5 to 1·7 times that of Scheme I. Also, Scheme II is economical from a high-speed memory storage point of view. For symmetric and positive-definite matrices F, care should be taken in selecting the value of the parameter μ to achieve convergence for Scheme II. Restrictions on μ to guarantee convergence, are provided in Udwadia and Kumar.[8]

APPENDIX

The damping matrix F for Example 1 is defined as

$$F = \begin{bmatrix} 1{\cdot}40 & 0{\cdot}10 & 0{\cdot}30 & 0{\cdot}08 & 0{\cdot}11 & 0{\cdot}16 & 0{\cdot}10 & 0{\cdot}21 & 0{\cdot}17 & 0{\cdot}09 \\ -0{\cdot}20 & 2{\cdot}30 & 0{\cdot}40 & -0{\cdot}10 & 0{\cdot}50 & 0{\cdot}10 & 0{\cdot}30 & -0{\cdot}12 & -0{\cdot}16 & 0{\cdot}28 \\ 0{\cdot}20 & 0{\cdot}30 & 2{\cdot}70 & 0{\cdot}20 & 0{\cdot}40 & 0{\cdot}30 & 0{\cdot}30 & -0{\cdot}02 & -0{\cdot}16 & 0{\cdot}24 \\ -0{\cdot}40 & 0{\cdot}10 & -0{\cdot}20 & 2{\cdot}40 & 0{\cdot}50 & 0{\cdot}40 & 0{\cdot}30 & 0{\cdot}10 & -0{\cdot}06 & 0{\cdot}11 \\ -0{\cdot}20 & 0{\cdot}50 & 0{\cdot}40 & -0{\cdot}10 & 2{\cdot}80 & 0{\cdot}10 & 0{\cdot}30 & -0{\cdot}12 & -0{\cdot}16 & 0{\cdot}28 \\ 0{\cdot}10 & 0{\cdot}40 & 0{\cdot}35 & 0{\cdot}15 & 0{\cdot}50 & 3{\cdot}10 & 0{\cdot}20 & 0{\cdot}22 & 0{\cdot}26 & 0{\cdot}18 \\ -0{\cdot}20 & 0{\cdot}40 & 0{\cdot}40 & -0{\cdot}10 & 0{\cdot}50 & 0{\cdot}10 & 2{\cdot}30 & -0{\cdot}12 & -0{\cdot}16 & 0{\cdot}28 \\ 0{\cdot}15 & -0{\cdot}35 & 0{\cdot}40 & 0{\cdot}10 & 0{\cdot}45 & -0{\cdot}15 & 0{\cdot}30 & 2{\cdot}52 & -0{\cdot}06 & 0{\cdot}38 \\ -0{\cdot}20 & 0{\cdot}30 & 0{\cdot}40 & -0{\cdot}10 & 0{\cdot}50 & 0{\cdot}10 & 0{\cdot}30 & -0{\cdot}12 & 3{\cdot}16 & 0{\cdot}28 \\ -0{\cdot}40 & -0{\cdot}09 & 0{\cdot}35 & -0{\cdot}18 & 0{\cdot}42 & 0{\cdot}14 & 0{\cdot}20 & -0{\cdot}22 & -0{\cdot}16 & 2{\cdot}28 \end{bmatrix} \tag{22}$$

and the modal stiffness matrix is given by

$$\Lambda = \text{diag}\,\{20{\cdot}0,\ 20{\cdot}0,\ 25{\cdot}0,\ 20{\cdot}0,\ 20{\cdot}0,\ 15{\cdot}0,\ 20{\cdot}0,\ 20{\cdot}0,\ 23{\cdot}0,\ 20{\cdot}0\} \tag{23}$$

with the initial conditions

$$z_i(0) = 1{\cdot}0 \quad \text{and} \quad \dot{z}_i(0) = 0{\cdot}0, \; i = 1, 2, 3, 4, 5, 6, 7, 8, 9, 10 \tag{24}$$

This system is subjected to the forcing function $h(t)$ given by

$$h_i(t) = 2 \sin \sqrt{20}t, \quad i = 1, 3, 5, 7, 9, 10$$

and (25)

$$h_i(t) = -2 \sin \sqrt{20}t, \quad i = 2, 4, 6, 8, \; t \in (0, 10)$$

The damping matrix F for Example 3 is[15]

$$F = \begin{bmatrix} 1{\cdot}35 & 0{\cdot}23 & 0{\cdot}11 & 0{\cdot}05 & 0{\cdot}05 & 0{\cdot}07 & 0{\cdot}07 & 0{\cdot}12 & 0{\cdot}23 & 0{\cdot}22 \\ 0{\cdot}23 & 1{\cdot}45 & 0{\cdot}24 & 0{\cdot}14 & 0{\cdot}10 & 0{\cdot}10 & 0{\cdot}17 & 0{\cdot}26 & 0{\cdot}30 & 0{\cdot}20 \\ 0{\cdot}11 & 0{\cdot}24 & 1{\cdot}46 & 0{\cdot}28 & 0{\cdot}18 & 0{\cdot}18 & 0{\cdot}27 & 0{\cdot}31 & 0{\cdot}19 & 0{\cdot}04 \\ 0{\cdot}05 & 0{\cdot}14 & 0{\cdot}28 & 1{\cdot}51 & 0{\cdot}36 & 0{\cdot}35 & 0{\cdot}32 & 0{\cdot}19 & 0{\cdot}05 & -0{\cdot}01 \\ 0{\cdot}05 & 0{\cdot}10 & 0{\cdot}18 & 0{\cdot}36 & 1{\cdot}67 & 0{\cdot}50 & 0{\cdot}26 & 0{\cdot}05 & -0{\cdot}01 & 0{\cdot}00 \\ 0{\cdot}07 & 0{\cdot}10 & 0{\cdot}18 & 0{\cdot}35 & 0{\cdot}50 & 1{\cdot}58 & 0{\cdot}23 & 0{\cdot}05 & 0{\cdot}01 & 0{\cdot}00 \\ 0{\cdot}07 & 0{\cdot}17 & 0{\cdot}27 & 0{\cdot}32 & 0{\cdot}26 & 0{\cdot}23 & 1{\cdot}37 & 0{\cdot}18 & 0{\cdot}07 & 0{\cdot}00 \\ 0{\cdot}12 & 0{\cdot}26 & 0{\cdot}31 & 0{\cdot}19 & 0{\cdot}05 & 0{\cdot}05 & 0{\cdot}18 & 1{\cdot}39 & 0{\cdot}18 & 0{\cdot}07 \\ 0{\cdot}23 & 0{\cdot}30 & 0{\cdot}19 & 0{\cdot}05 & -0{\cdot}01 & 0{\cdot}01 & 0{\cdot}07 & 0{\cdot}18 & 1{\cdot}39 & 0{\cdot}17 \\ 0{\cdot}22 & 0{\cdot}20 & 0{\cdot}04 & -0{\cdot}01 & 0{\cdot}00 & 0{\cdot}00 & 0{\cdot}00 & 0{\cdot}07 & 0{\cdot}17 & 1{\cdot}32 \end{bmatrix} \tag{26}$$

REFERENCES

1. T. K. Caughey, 'Classical normal modes in damped linear structures', *J. appl. mech. ASME* **27**, 269–271 (1960).
2. T. K. Caughey and M. J. O'Kelly, 'General theory of vibrations of damped linear dynamic systems', *Report of the Dynamics Laboratory*, California Institute of Technology, Pasadena, CA, 1963.
3. F. E. Udwadia and R. S. Esfandiari, 'Nonclassically damped dynamic systems: an iterative approach', *J. appl. mech. ASME* **57**, 423–433 (1990).
4. S. M. Shahruz and G. Langari, 'Closeness of the solutions of approximately decoupled damped linear systems to their exact solutions', *Report No. ESRC91-10*, University of California, Berkeley, CA, 1991.
5. S. M. Shahruz and A. K. Packard, 'Approximate decoupling of weakly nonclassically damped linear second-order systems under harmonic excitations', *Report No. ESRC91-11*, University of California, Berkeley, CA, 1991.
6. S. F. Felszeghy, 'On uncoupling and solving the equations of motion of vibrating linear discrete systems', *J. appl. mech. ASME* (to appear).
7. A. M. Clart and F. Venancio-Filho, 'A modal superposition pseudo-force method for dynamic analysis of structural systems with non-proportional damping', *Earthquake eng. struct. dyn.* **20**, 303–315 (1991).
8. F. E. Udwadia and R. Kumar, 'Convergence of iterative methods for non-classically damped dynamic systems', to appear in *Appl. math. comput.* **61**, No. 1, (1994).
9. P. E. Duncan and R. Eatock Taylor, 'A note on the dynamic analysis of non-proportionally damped systems', *Earthquake eng. struct. dyn.* **7**, 99–105 (1979).
10. T. K. Hasselman, 'Modal coupling in lightly damped structures', *AIAA j.* **14**, 1627–1628 (1976).
11. W. H. Press, B. P. Flannery, S. A. Teukolsky and W. T. Vetterling, *Numerical Recipes*, Cambridge University Press, Cambridge, 1986.
12. N. Nigam and P. C. Jennings, 'Digital calculation of response spectra from strong motion earthquake records', *EERL Report No. 700-00*, California Institute of Technology, Pasadena, CA, 1968.
13. G. B. Warburton and S. R. Soni, 'Errors in response calculations for non-classically damped structures', *Earthquake eng. struct. dyn.* **5**, 365–371 (1977).
14. R. S. Varga, *Matrix Iterative Analysis*, Prentice-Hall, Englewood Cliffs, NJ, 1963.
15. K. J. Bunch and R. W. Grow, 'A simple method to generate test matrices of known eigenvalue or singular value spectra', *Comput. math. appl.* **22**, 65–67 (1991).